











BrainFuseNet: Enhancing Wearable Seizure Detection Through EEG-PPG-Accelerometer Sensor Fusion and Efficient Edge Deployment

Thorir Mar Ingolfsson , Graduate Student Member, IEEE, Xiaying Wang , Member, IEEE, Upasana Chakraborty , Simone Benatti , Member, IEEE, Adriano Bernini , Pauline Ducouret , Philippe Ryvlin , Sándor Beniczky , Luca Benini , Fellow, IEEE, and Andrea Cossetti , Member, IEEE

Abstract—This paper introduces BRAINFUSENET, a novel lightweight seizure detection network based on the sensor fusion of electroencephalography (EEG) with photoplethysmography (PPG) and accelerometer (ACC) signals, tailored for low-channel count wearable systems. BRAINFUSENET utilizes the Sensitivity-Specificity Weighted Cross-Entropy (SSWCE), an innovative loss function incorporating sensitivity and specificity, to address the challenge of heavily unbalanced datasets. The BRAINFUSENET-SSWCE approach successfully detects 93.5% seizure events on the CHB-MIT dataset (76.34% sample-based sensitivity), for EEG-based classification with only four channels. On the PEDESITE dataset, we demonstrate a sample-based sensitivity and false positive rate of 60.66% and 1.18 FP/h, respectively, when considering EEG data alone. Additionally, we demonstrate that integrating PPG signals increases the sensitivity to 61.22% (successfully detecting 92% seizure events) while decreasing the number of false positives to 1.0 FP/h. Finally, when ACC data are also considered, the sensitivity increases to 64.28% (successfully detecting 95% seizure events) and the number of false positives drops to only 0.21 FP/h for sample-based estimations, with less than one false alarm per day when considering event-based estimations. BRAINFUSENET is resource-friendly and well-suited for implementation on low-power embedded platforms, and we

evaluate its performance on GAP9, a state-of-the-art parallel ultra-low power (PULP) microcontroller for tiny Machine Learning applications on wearables. The implementation on GAP9 achieves an energy efficiency of 21.43 GMAC/s/W, with an energy consumption per inference of only 0.11 mJ at high performance (412.54 MMAC/s). The BRAINFUSENET-SSWCE method demonstrates effective and accurate seizure detection on heavily imbalanced datasets while achieving state-of-the-art performance in the false positive rate and being well-suited for deployment on energy-constrained edge devices.

Index Terms—Epilepsy, seizure detection, embedded deployment, sensor fusion, wearable devices.

I. INTRODUCTION

EPILEPSY is a widespread neurological disorder that affects over 50 million individuals globally and is characterized by recurrent seizures that disrupt cerebral function [1]. While traditional treatments primarily revolve around pharmacological interventions, instances of pharmacoresistance necessitate alternative approaches like surgical interventions or neurostimulation [2]. This underscores the imperative for personalized treatments and comprehensive brain activity monitoring [3]. The common monitoring approach requires hospitalization in an epilepsy monitoring unit (EMU), where video surveillance and noninvasive Electroencephalography (EEG) caps (typically with 32 or 64 channels) are used to classify various seizure types, given that generalized convulsive seizures are relatively rare [4], [5], [6]. However, a critical need remains for advanced, long-term, ambulatory monitoring solutions to assess seizure frequency and enable seizure-triggered alert systems.

The evolution of EEG-based seizure detection in wearable technologies is pivotal in overcoming the limitations of conventional EEG systems, which are often perceived as burdensome and stigmatizing. The transition to wearable devices is driven by the need for discreet, long-duration, user-friendly monitoring systems for patients and caregivers. These devices, incorporating machine learning algorithms, facilitate prompt intervention and provide clinicians with valuable data to refine antiepileptic treatments. Nonetheless, developing effective wearable seizure detection systems faces significant challenges [7].

First of all, resources are limited in wearable settings, and it is crucial to balance accuracy with miniaturization and

Manuscript received 21 February 2024; revised 15 April 2024; accepted 21 April 2024. Date of publication 30 April 2024; date of current version 13 August 2024. This work was supported in part by the Swiss National Science Foundation (Project PEDESITE) under Grant Agreement 193813 and in part by the ETH-Domain Joint Initiative program (project UrbanTwin). This paper was recommended by Associate Editor M. Atef. (Xiaying Wang and Upasana Chakraborty contributed equally to this work.) (Corresponding author: Thorir Mar Ingolfsson.)

Thorir Mar Ingolfsson, Upasana Chakraborty, and Andrea Cossetti are with the Integrated Systems Laboratory, ETH Zürich, 8092 Zürich, Switzerland (e-mail: thoriri@iis.ee.ethz.ch).

Xiaying Wang is with the Integrated Systems Laboratory, ETH Zürich, 8092 Zürich, Switzerland, and also with the Swiss University of Traditional Chinese Medicine, 5330 Bad Zurzach, Switzerland.

Simone Benatti is with the DISMI, University of Modena and Reggio Emilia, 41121 Reggio Emilia, Italy, and also with the DEI, University of Bologna, 40126 Bologna, Italy.

Adriano Bernini, Pauline Ducouret, and Philippe Ryvlin are with Lausanne University Hospital (CHUV), 1011 Lausanne, Switzerland.

Sándor Beniczky is with Aarhus University Hospital, 8200 Aarhus, Denmark, and also with the Danish Epilepsy Centre (Filadelfia), 4293 Dianalund, Denmark.

Luca Benini is with the Integrated Systems Laboratory, ETH Zürich, 8092 Zürich, Switzerland, and also with the DEI, University of Bologna, 40126 Bologna, Italy.

Color versions of one or more figures in this article are available at <https://doi.org/10.1109/TBCAS.2024.3395534>.

Digital Object Identifier 10.1109/TBCAS.2024.3395534

energy efficiency for extended battery life. Recent developments in smart edge computing, particularly with low-power microcontrollers, offer viable solutions to these challenges [8]. Such advancements enable extended device operation and efficient AI model execution [9]. However, aligning AI algorithms with the limited computational capacities of wearable devices remains a significant hurdle, requiring careful model selection and optimization for effective deployment on these low-power platforms.

Secondly, optimizing performance in terms of sensitivity is not sufficient: minimizing false alarms is paramount in long-term monitoring, as their prevalence can erode users' trust and hinder the adoption of the technology [10]. Therefore, prioritizing specificity, even when missing some seizures, is vital for user confidence and device adherence.

Another significant challenge lies in adapting AI models, traditionally reliant on large-count electrode arrays, to maintain accuracy in wearables with a small number of channels. While recent systems demonstrate high sensitivity and specificity [11], translating them to wearable form factors requires innovative approaches to maintain performance.

Furthermore, there are considerable differences in the EEG seizure patterns based on type, etiology, and individual brain characteristics [12], [13]. Such patient variability underscores the need for personalized models. Tailoring models to individual patients can significantly enhance detection accuracy and device efficiency, thereby improving therapeutic outcomes [14], [15].

Finally, compared to other biosignals, EEG presents a low signal-to-noise ratio and, especially in the context of wearables, is especially prone to artifacts [16]. On top of that, some seizure types are elusive to EEG alone [17]. As such, successful and reliable seizure detection should aim for multi-modal approaches, exploiting information from heterogeneous sensors. Such multi-modal approach can be envisioned to rely on multiple, heterogeneous devices, synchronized to each other in a body area network for concurrent data acquisitions. In this context, integrating plethysmography (PPG) sensors with EEG has enhanced biosignal analysis accuracy and broadened its scope [18], [19], especially for enhancing seizure detection sensitivity in ambulatory settings [20]. However, more exploration is needed to assess the influence of wrist-based signals in detecting seizures and reducing false alarms when combined to EEG.

This paper¹ addresses all the above challenges by introducing BRAINFUSENET, a novel network for seizure detection via sensor fusion of EEG with PPG and Accelerometer (ACC) signals, aimed at minimizing false positives while retaining high sensitivity to seizure events, tailored for low-channel count wearable systems, trained with a subject-specific approach on a recent heterogeneous seizure dataset, and featuring low memory requirements and power consumption for optimal deployment on edge devices.

¹This work is an extension of our previous conference paper [21], where we introduced the EPIDENET architecture and the Sensitivity-Specificity Weighted Cross Entropy (SSWCE) loss function.

II. RELATED WORKS

A. Wearable Technologies in Epilepsy Management

The advent of wearable technologies marks the beginning of a transformative era in epilepsy management. Initially, EEG systems were confined to clinical settings due to their size and complexity. However, the past decade has seen a paradigm shift toward the development of compact, user-friendly wearable devices designed for continuous monitoring.

These wearable technologies integrate advanced biosensors, including EEG and PPG, facilitating long-term, ambulatory seizure monitoring without significant intrusion into daily life [22]. The ongoing incorporation of machine learning algorithms into these devices is significantly improving their ability to detect seizures accurately and in real-time, greatly benefiting users [23].

Furthermore, wearable technologies have improved patient autonomy and quality of life. By providing discreet monitoring, these devices reduce the stigma and psychological burden associated with traditional EEG systems [24]. Moreover, they enable proactive management of epilepsy, allowing for timely intervention and potentially reducing seizure-related risks.

To develop systems that can be worn without stigma in everyday activities, system design for seizure monitoring focuses on devices like wristbands, headbands, earbuds, and eyeglasses. For instance, Empatica E4 and Embrace2 [25], FDA-approved wristbands, stand out for their ability to monitor EDA and motion, as well as heart rate and temperature, offering real-time seizure detection by virtue of a data link with cloud servers which execute the parameter monitoring and alert users and their caregivers in case of seizure onsets [26]. Another noteworthy example is the Neurovigil iBrain [27], a headband that captures high-resolution EEG data to facilitate sleep studies and potentially detect seizures during sleep. On the research front, projects like Seer Medical's wearable EEG system [28] are pushing the boundaries by offering a portable, head-mounted device that provides continuous EEG monitoring outside clinical settings.

Innovative strides have also been made with the development of smart eyeglasses. These devices embody the cutting edge of discreet, real-time seizure monitoring. Smart glasses, which integrate EEG electrodes into their frame for continuous EEG monitoring, provide a non-invasive and inconspicuous platform for wearable seizure detection systems. Although still in the experimental or conceptual stages, such eyewear aims to utilize visual cues and physiological data to alert users of impending seizures, ensuring both functionality and fashion. This integration of technology into everyday objects underscores the commitment to creating wearables that advance medical care and cater to the lifestyle of individuals with epilepsy [8], [29].

Another potentially groundbreaking solution is represented by earbuds with EEG sensors. Several works, like [30], have demonstrated the feasibility of integrating EEG sensors into earbuds or earpieces. These studies aim to validate the accuracy of EEG data collected from the ear canal, which is relatively close to the brain and could offer a less intrusive alternative to traditional scalp-based EEG systems. These devices are mostly

at the research stage [31], even though there are some attempts to bring them into commercial products [32].

In summary, multiple heterogeneous technologies are currently under development for wearable epilepsy monitoring, and they are typically based on a reduced number of sensor channels. All these alternative sensing solutions are ultimately envisioned to be integrated in body area networks featuring multiple sensing nodes connected to each other wirelessly at low power [33], [34]. In this context, this work also focuses on reduced channel count applications, with heterogeneous sensor data from the head (EEG) and the wrist (PPG, ACC).

B. The Need for Artifacts and False Alarms Reduction

Despite the significant advancements in wearable technologies for epilepsy management, several challenges and limitations remain. One major issue is the accuracy and specificity of seizure detection algorithms. False positives and negatives continue to pose a significant challenge, impacting patient trust and the clinical utility of these devices [35]. In this context, artifacts appear as the main source of false positive detection, and recent studies have dedicated efforts to address these challenges. The work in [36] demonstrates how implementing artifact detection before doing seizure detection can significantly reduce false alarm rates in seizure detection models. Frolich et al. [37] also explored linear decomposition methods to mitigate the impact of muscle movement artifacts in EEG recordings. In the realm of PPG, Al-Sheikh [38] investigated adaptive algorithms capable of compensating for motion-induced noise, illustrating a marked improvement in signal fidelity. Additionally, sensor fusion between heterogeneous signal sources also demonstrated remarkable potential for reducing false positive detections [39]. In addition, the integration of EEG with other biosignals, such as Electrocardiogram (ECG), Electrodermal Activity (EDA), and PPG, has shown great promise in detecting subtle seizure types that may not be easily identifiable through EEG alone [40].

In this work, we also focus on the minimization of false positive detections by exploiting EEG-PPG-ACC sensor fusion approaches.

C. Algorithms for Wearables

Striking a balance between accuracy and usability in wearable devices requires the development of algorithms for seizure detection in systems with a low channel count. These algorithms, tailored for sparse EEG data, employ advanced machine learning and deep learning techniques to overcome the challenges presented by limited inputs. Moreover, the continuous and fast evolution of such algorithms and use cases, as well as the opportunity to adapt models on a subject-specific basis, requires the wearable platform to be highly adaptable and flexible in computation. In this regard, general-purpose yet low-power MCUs provide the best tradeoff [41]. Application specific integrated circuits (ASICs) [42], [43], [44], [45] can achieve much lower power consumption, but they lack

flexibility, which is essential in the current research context, as the challenge of artifact removal and false positive reduction below the patient acceptability threshold is still open and requires further algorithmic research and development. Techniques such as support vector machines (SVM) [46], K-Nearest Neighbour (KNN) [47], AdaBoost [48], and Energy-based algorithms [49] have been successful in extracting relevant features from EEG signals—ranging from frequency and time-domain characteristics to statistical insights—essential for distinguishing seizures from normal brain activity despite the reduced spatial data from fewer channels. Nevertheless, many of these papers show a significant decline in accuracy and sensitivity/specificity performance, creating the need for refining algorithms to perform efficiently with minimal channel count.

Recent works based on low channel-count seizure detection demonstrated significant reductions in the false positive rates. One relevant example is offered by Vandecasteele et al. [50], who achieved less than 1 FP/h with 63.4% sensitivity on a dataset with 54 subjects, when using only 4 EEG channels and an SVM classifier.

Another example is given by Busia et al. [51], [52], who proposed a transformer-based architecture (EEGFormer), detecting 73% of seizure events with less than 1 FP/h on the CHB-MIT dataset. However, the reported performance was obtained only on a selected subset of the patients available in the dataset. When applied on the PEDESITE dataset, 88% of seizure events have been detected with less than 0.5 FP/h. Despite the significant improvements, further work is needed to bring the false alarms to less than one per day.

In exploring wearable technologies for epilepsy monitoring, Mohammadpour et al. [53] conducted a seminal study assessing the feasibility of using photoplethysmography (PPG) for seizure detection. This research, involving 174 patients from the epilepsy monitoring unit at Boston Children's Hospital, focused on analyzing PPG signals during baseline, pre-seizure, and post-seizure periods. Key observations included an increase in PPG frequency and changes in slope and smoothness, underscoring the potential of PPG as a non-invasive biomarker for seizure detection systems.

Zambrana et al. [20] further advanced the field with a novel seizure predictive model combining Ear EEG, ECG, and PPG signals. Their model, versatile for use in both static and outpatient settings, showed promising results with an accuracy of 91.5% and sensitivity of 85.4%. However, the study lacked detailed analysis on false positives per hour (FP/h) and latency.

Vandecasteele et al. [54] compared wearable ECG and PPG devices against hospital ECG for seizure detection in TLE patients. The wearable ECG showed higher sensitivity (70%) compared to hospital ECG (57%) and wrist-worn PPG device (32%), suggesting the potential of wearable ECG for long-term seizure monitoring.

In this work, we tackle the challenge of lightweight multi-sensor models, demonstrating for the first time EEG+PPG+ACC seizure detection on edge-computing devices with state-of-the-art performance (quantitative comparisons are provided in the Results section).

D. Imbalanced Datasets and Loss Functions

When developing algorithms for seizure detection, Cross-Entropy (CE) loss is a widely used loss function. However, its effectiveness is often compromised in imbalanced datasets, a common scenario in epilepsy research, where the disparity in class distributions can lead to biased predictions by the model.

Several alternative loss functions and techniques have been explored to address the challenges posed by imbalanced datasets. As introduced by Lin et al. in 2017 [55], Focal Loss modifies the CE loss to apply a focusing parameter to down-weight easy examples and thus focus training on hard negatives. This approach proves beneficial in scenarios with an imbalance between foreground and background classes, as it prevents the overwhelming number of easy negatives from dominating the gradient.

Weighted Cross-Entropy (WCE) Loss, described by Wang et al. in 2016 [56], assigns different weights to classes in the loss function. This strategy is particularly effective in datasets where some classes are underrepresented, as it amplifies the error signal from the minority class, thereby pushing the model to pay more attention to these classes.

Oversampling and undersampling techniques, such as those discussed by Chawla et al. in 2002 [57] and Drummond et al. in 2003 [58], aim to balance the class distribution either by increasing the number of instances in the minority class (oversampling) or reducing the instances in the majority class (undersampling). These techniques alter the dataset to create a more balanced class distribution, facilitating more effective learning.

Ingolfsson et al. [21] proposed incorporating domain-specific knowledge into the loss function to overcome the limitations of CE loss. The proposed Sensitivity-Specificity Weighted Cross-Entropy (SSWCE) loss incorporates both sensitivity and specificity into the CE loss, allowing for the adjustment of the loss function to prioritize either specificity or sensitivity and effectively balancing the two metrics in the training process, addressing the bias towards the majority class commonly seen in imbalanced datasets.

This work also makes use of the SSWCE loss.

III. METHODS

A. Datasets

This work leverages the CHB-MIT public dataset and the dataset collected in the PEDESITE study. Table I summarizes their structure.

The CHB-MIT dataset [59] comprises EEG data from 23 pediatric and young adult patients (aged 1.5–22 years) with intractable seizures, collected at 256 samples per second and a 16-bit resolution with a 10/20 system. We process this dataset considering 4 second windows, which equates to $T_E = 1024$ EEG time samples.

Recognizing the CHB-MIT dataset’s limitations in real-world scenarios (pediatric patients, gaps in the EEG traces, nearly zero artifacts), we also evaluate our approach using the PEDESITE dataset. The PEDESITE study took place during routine clinical evaluations at several in-hospital epilepsy monitoring units in Switzerland and Denmark, where patients are

TABLE I
SUMMARY OF THE EMPLOYED DATASETS

Patient	No. Seizures [†]	Recording Duration	Avg. Seiz. Length (s)
CHB-MIT			
chb01	7	1d 17h 33min	63.14
chb02	3	1d 11h 16min	57.33
chb03	7	1d 14h 2min	57.43
chb04	4	6d 7h 6min	94.50
chb05	5	2d 15h 12min	111.60
chb06	10	2d 18h 45min	153.60
chb07	3	2d 19h 5min	108.30
chb08	5	1d 2h 19min	183.80
chb09	4	2d 19h 52min	69.00
chb10	7	2d 2h 2min	63.86
chb11	3	1d 9h 45min	268.70
chb12	27* (40)	21h 41min	36.63
chb13	12	11h 0min	44.00
chb14	8	1d 2h 0min	211.12
chb15	20	1d 15h 1min	99.60
chb16	10	17h 1min	8.62
chb17	3	20h 1min	97.67
chb18	6	1d 10h 43min	52.83
chb19	3	1d 4h 53min	78.67
chb20	8	1d 3h 40min	36.75
chb21	4	1d 8h 23min	49.75
chb22	3	1d 8h 0min	64.00
chb23	7	1d 2h 36min	60.57
chb24	16	22h 17min	31.94
Total	185	43d 0h 16min	-
PEDESITE			
P1	3 (3)	(EEG) 4d 10h 59min (PPG)** 3d 6h 58min	488
P2	7 (5)	(EEG) 3d 20h 32min (PPG+ACC) 3d 7h 57min	64.86
P3	5 (5)	(EEG) 2d 21h 58min (PPG+ACC) 2d 21h 7min	117.20
P4	3 (3)	(EEG) 3d 20h 13min (PPG+ACC) 3d 15h 57min	117.98
P5	4 (4)	(EEG) 3d 18h 23min (PPG+ACC) 3d 20h 7min	35.25
P6	3 (3)	(EEG) 5d 19h 23min (PPG+ACC) 7d 6h 10min	118.67
Total	25 (23)	(EEG) 23d 1h 28min (PPG+ACC) 24d 6h 16min	-

[†] For PEDESITE: not all seizures are captured by wrist data; the number of seizures recorded both by EEG and wrist data is between brackets.

*Only 27 seizures of 40 are considered for chb12 since channels change in subsequent recordings (hence, as total number of seizures we considered 185 instead of 198)

**Patient P1 does not have ACC data.

hosted to record and characterize their epileptic seizures. Before the start of the monitoring, 24 Compumedics disposable Ag/AgCl sintered electrodes are fixed to the patient’s scalp. Afterwards, these electrodes are connected to an amplifier and then converted from analog to digital signals (SD LTM PLUS 64²). Healthcare professionals monitor brain activity in real-time, coupled with the video, electrocardiogram, and pulse oximetry signals. Patient monitoring ranges from a minimum of two consecutive days to a maximum of two weeks. Scalp-EEG signals are collected at 1024 samples per second and a 16-bit resolution with a 10/20 system. Monitoring durations

²<https://micromedgroup.com/products/brainquick/brainquick-ltm/>

range from 2 days to two weeks. We further decimate the signal to 256 samples per second, to be comparable to the sampling rate of CHB-MIT, and look at 8 second windows, which correspond to $T_E = 2048$ EEG time samples. The selection of the optimal window size is dataset-dependent, and the choice is based on our previous analysis [36], where we have determined these specific windows to be optimal for minimizing false positives while maintaining a balance between sensitivity and specificity.

In addition to EEG monitoring, in the PEDESITE study, patients were also equipped with the E4 wristband by Empatica, which incorporates a PPG sensor for heart rate monitoring and an integrated ACC. The PPG data is sampled at 64 samples per second and we look at 8 second windows, which equates to $T_P = 512$ PPG time samples. The ACC data is instead sampled at 32 samples per second. Unless otherwise stated, in the following, we will use the terminology “wrist data” for referring to PPG and ACC together. When PPG and ACC data are considered together, PPG data are downsampled (see Sect. III-E), and 8 second windows of wrist data equate to $T_W = 256$ samples.

The PEDESITE study obtained approval for retrospective data analysis with a waiver of informed consent (due to the retrospective nature of the study) from the local Ethical Committee of the University of Lausanne (study nr 2021-01419). The study report conforms to the STROBE statement for the report of observational cohort studies. All the methods are in accordance with institutional guidelines and regulations.

B. Subject-Specific Training and Cross-Validation Approach

We follow a subject-specific training approach, in alignment with the findings of previous research [21], [60]. This subject-specific paradigm entails that each model is trained using data exclusively derived from the respective subject. This ensures that the model is finely tuned to each individual’s unique characteristics and seizure patterns, potentially leading to enhanced performance in seizure detection.

To augment the robustness of the performance metrics obtained for each model, we also follow a Leave-One-Out Cross-Validation (LOOCV) strategy at record-level, i.e., we train the model on all records (of one subject) that contain seizure events except for one, utilizing the excluded record for validation purposes. We iteratively repeat this process, each time excluding a different record, to ensure a comprehensive coverage and evaluation of the model’s performance across the entire dataset. Importantly, at the start of each iteration, a new instance of the neural network is initialized with random weights, eliminating any potential for validation data leakage across iterations and ensuring no single network iteration is exposed to the entirety of the data.

Moreover, to account for variability of the training process and reinforce the reliability of our findings, each metric is reported as the average of five repeated runs, each conducted with a distinct random seed. Averaging over multiple runs mitigates anomalies or biases that might arise from a

single iteration, yielding a more representative measure of the model’s performance.

C. Sensitivity-Specificity Weighted Loss Function and Smoothing

To address the challenge of imbalanced datasets (see Sect. II-D), in our previous publication [21] we proposed incorporating domain-specific knowledge into the loss function, as defined in Equation (1), by introducing the SSWCE loss, which incorporates both sensitivity (SN) and specificity (SP) into the CE loss:

$$SSWCE(y, p) = CE(y, p) + \alpha(1 - SP) + \beta(1 - SN) \quad (1)$$

In this equation, y represents the true class label (0 or 1), and p is the predicted probability of the positive class (1). The hyperparameters α and β are user-defined, allowing for the adjustment of the loss function to prioritize either specificity or sensitivity. This approach effectively balances sensitivity and specificity in the training process, addressing the bias towards the majority class commonly seen in imbalanced datasets.

In [21], we utilized the SSWCE loss function to modulate either sensitivity or specificity independently. This was achieved through a comprehensive grid search to ascertain the most effective combination of the hyperparameters α and β for individual patients within the PEDESITE dataset. Building up from the results of [21], in this paper we further extend the analysis by also considering the CHB-MIT dataset, which features a larger patient population. By including this dataset in our grid search for the optimal α and β parameter combination, we aim to validate and potentially refine our previous findings, enhancing the generalizability and applicability of the SSWCE loss function across a wider patient demographic, thereby contributing to the robustness and precision of our model in diverse clinical settings.

In addition, we also considered three-window majority voting for smoothing classification outputs (hereby referred to as “smooth”) [60]. Smoothing reduces false positives by considering the predictions of adjacent windows (N-1 and N+1) alongside the current window (N). Window N is marked as having a seizure event only if at least two out of these three windows suggest a seizure. This approach enhances specificity by filtering out isolated false positives [21], which are unlikely to be actual seizures due to their short duration.

D. Seizure Detection Utilizing EEG Data Only

The model architecture to process EEG data is EpiDENET, introduced in our previous work of [60] and shown in Fig. 1 (the EEG block, followed by the FCN of size 2). The architecture is engineered to learn and extract salient features from the input dataset sequentially. In its preliminary layers, the network is primed to discern frequency filters, for delineating the spectral attributes of the dataset. Progressing to the intermediary layers, the focus shifts to deriving spatial filters specific to particular frequency bands, enabling the model to identify spatial patterns influenced by distinct frequency ranges. Finally, a dense layer

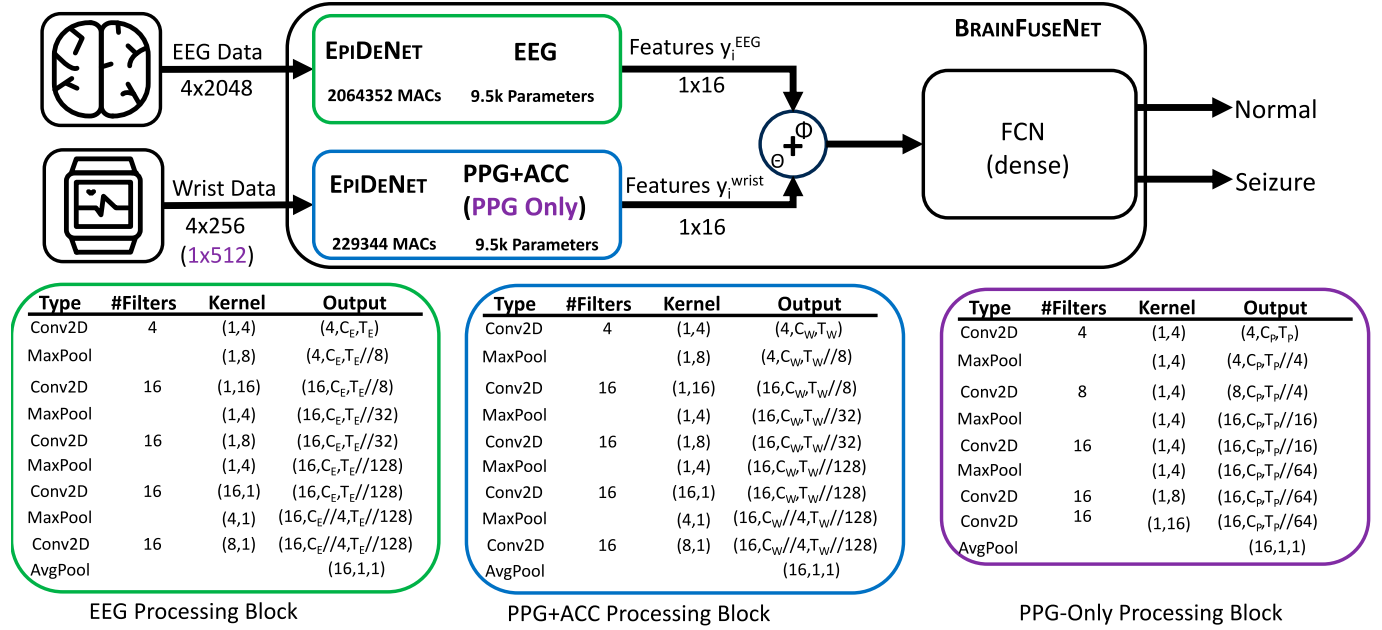


Fig. 1. Representation of the BRAINFUSENET framework for combined EEG and PPG/ACC classification. EEG data (4 channels, 2048 samples) are fed to an EPIDeNET model (green box), which generates 16 EEG features y_i^{EEG} . Similarly, PPG+ACC data (1 channel PPG, 3 channels ACC, 256 samples) are fed to an EPIDeNET model (blue box), which generates 16 wrist features y_i^{wrist} . The outputs of the EEG and PPG+ACC blocks are summed (with weights Φ and Θ , respectively) into a comprehensive feature vector, which then serves as the input for the FCN. The FCN classifies normal vs seizure activity. If ACC data are not used, the PPG+ACC block is replaced by a PPG-only block (purple box), and PPG data do not need to be downsampled (i.e., the input from wrist data becomes of 1 channel with 512 samples). Symbols definition: C_E = EEG channels, T_E = EEG time samples, C_W = wrist channels, T_W = wrist time samples, C_P = PPG channels, T_P = PPG time samples.

combines the feature maps generated by the upstream layers. This approach enhances the model's ability to classify and predict results in complex scenarios.

This paper uses EPIDeNET for the analyses based on EEG data alone, on the CHB-MIT and PEDESITE datasets. We limit the number of channels to 4 (in the temporal region) in alignment with the reduced number of channels available in wearable devices. Furthermore, we use and adapt EPIDeNET also for other biosignals and for sensor fusion (see the following sections).

E. Seizure Detection Utilizing Wrist Data Only

To evaluate the seizure detection performance when relying exclusively on data acquired from a wrist-worn device (PPG and ACC), we explored three approaches (all limited to the PEDESITE dataset).

1) *Employment of Solely PPG Data:* The PPG signal, acquired at a sampling rate of 64Hz from the wristband device, serves as the sole input to a modified version of the EPIDeNET architecture, which is adapted to accommodate a single-channel input as opposed to the original four-channel configuration (we use the PPG block of Fig. 1, followed by the FCN of size 2). This adaptation facilitates the analysis of 8-second segments of PPG data (we use 8 second windows to match the window size used for EEG data), equivalent to 512 data points, to evaluate the feasibility of seizure detection using PPG data in isolation.

2) *Integration of PPG and ACC Data at the Data Level:* Given the different sampling rates of PPG (64Hz) and ACC

(32Hz) data streams obtained from the wristband, to perform a data-level fusion, we decimate the PPG data to align with the ACC data's lower sampling frequency. Subsequently, the synchronized data is input into an EPIDeNET network (the PPG+ACC block of Fig. 1, followed by the FCN of size 2), mirroring the methodology employed for processing four-channel EEG data (using one channel for the PPG data and three channels for the 3-axes of ACC). This strategy aims to investigate the potential enhancement in seizure detection accuracy through the combined analysis of PPG and ACC data.

3) *Reconstructed PPG Data:* We use acceleration data along three axes (3-axes ACC data) to differentiate between uncontaminated and corrupted signal segments. Initially, the mean value is subtracted from the data corresponding to each accelerometer axis to mitigate baseline drift. Subsequently, we compare this adjusted data to a predetermined threshold (empirically evaluated). Should the magnitude of the data from any axis surpass this threshold, it is inferred that significant movement occurred within the corresponding timeframe, potentially compromising the PPG signal integrity, and the PPG signal undergoes a reconstruction process (as delineated below). If the magnitude of the data is below the threshold for all axes, the original PPG signal is maintained. The threshold parameter is subject to individual variability, necessitating adjustment on a per-patient basis. Specifically, a threshold of 0.02 is applied for patients exhibiting a high frequency of corrupted signal segments, whereas a more lenient threshold of 0.1 is adopted for the remainder. Following this preliminary filtration, the corrupted

signal segments are reconstructed via a wavelet-based approach as follows:

- The signal is disassembled into a hierarchy of *approximation* and *detail* coefficients through the application of Stationary Wavelet Transforms [61]. We explore 9, 10, and 11 decomposition levels, corresponding to temporal segments of 8, 16, and 32 seconds, respectively.
- While the *approximation* coefficients are preserved in their original state to maintain the signal’s overarching structure, the *detail* coefficients are cleaned by applying a parameter (denoted as δ) that removes the coefficients belonging to the motion artifacts. The δ value is set at 0.01 based on empirical tests, mirroring the protocol delineated in [62].
- These cleaned *detailed* coefficients are then used along with the original *approximate* coefficients to reconstruct the time domain PPG signal using the Inverse Stationary Wavelet transform.

This approach acknowledges the intrinsic variability of PPG signals across individuals, underscoring the necessity for patient-specific adjustment of reconstruction hyperparameters.

As for the PPG-only analyses, the network used to classify reconstructed PPG is again the PPG-only block of Fig. 1 plus the FCN of size 2 at the end.

F. Sensor Fusion of EEG With Wrist Data

A major distinction between Early Fusion and Late Fusion pertains to the juncture at which the model-derived features are amalgamated—either at the feature level (Early Fusion) or at the logits level (Late Fusion). This section elucidates the various fusion methodologies employed in our study to combine EEG with wrist data. These analyses are limited to the PEDESITE dataset, which comprises EEG and PPG/ACC data modalities.

1) *Early Fusion*: Early-fusion can be performed at data-level or feature-level. An example of data-level fusion between EEG and ECG is represented by [63], where Gabor functions are used for the fusion task on biosignals acquired with the same sampling frequency. Considering the difference in sampling frequency between EEG and wrist data in the PEDESITE dataset, we focus on feature-level early fusion to avoid excessive downsampling of EEG. Let us consider y_i^{EEG} and y_i^{wrist} to represent the feature sets extracted via convolutional neural network (CNN) models tailored for EEG and wrist data, respectively. In the context of early fusion, these features are amalgamated into a unified feature block denoted as $y_i^f = f(y_i^{EEG}, y_i^{wrist})$. We tested two approaches for feature combination:

- *Weighted Summation (Sum)*: feature sets from EEG and wrist data are summed as $y_i^f = \phi y_i^{EEG} + \theta y_i^{wrist}$, where ϕ and θ are parameters optimized concurrently through the network’s training, facilitating a dynamic weighting of features based on their relative importance.
- *Concatenation (Concat)*: the unified feature block corresponds to $y_i^f = [y_i^{EEG}, y_i^{wrist}]$, with feature vectors from each distinct CNN model being concatenated.

The concatenated array is subsequently input into a fully connected layer.

2) *Late Fusion*: Late Fusion is also known in the literature as *Decision-Level*, *Logits-Level*, or *Probability-Level* fusion. In decision or late-level fusion, CNNs are constructed to ensure that their terminal layers are fully connected layers, thereby outputting logits. These logits are subsequently integrated employing a fusion function denoted as $z_i^f = f(z_i^{EEG}, z_i^{wrist})$, following two alternative methodologies:

- *Weighted Summation*: Similarly to the weighted summation technique employed in Early Fusion, for Late Fusion we consider $z_i^f = \phi z_i^{EEG} + \theta z_i^{wrist}$, where ϕ and θ represent parameters refined through the network’s training process.
- *Rule Based Fusion*: this alternative strategy for amalgamating predictive insights from dual sensors involves leveraging the probabilities level. We consider a ‘Rule-Based Integration’ approach, where the ultimate prediction probability is exclusively derived from the EEG or wrist modalities. Despite making use of only one signal source at a time, it is still referred to as a Late Fusion approach in light of the need to compute and compare the prediction probabilities from both sensing modalities [64]. We evaluate the predictive outcomes produced by EEG and wrist independently on the validation dataset, utilizing these insights to establish a criterion for selecting the probability from either EEG or wrist as the definitive prediction probability. This ‘Rule-Based Integration’ modality inherently accords priority to one modality over another, predicated on the reliability of their predictive outcomes, and mitigates discrepancies or incongruities arising from disparate data sources.

G. BRAINFUSENET Model Architecture

Fig. 1 shows our proposed architecture for the EEG-PPG-ACC combined model, which incorporates dual network blocks based on EPIDENET. EEG data (4 channels, 2048 samples) are fused with wrist data (1 PPG channel and 3 ACC channels, 256 samples³) by summing the feature outputs of the EEG and PPG+ACC blocks into a comprehensive feature vector. This vector then serves as the input for a fully connected layer (FCN), producing the predictive outcome. Such an integrative approach significantly enhances the model’s proficiency in classifying and predicting outcomes in multifaceted situations. This network is referred to as BRAINFUSENET.

In the following, we also explore sensor fusion based on EEG+PPG only (hence, without ACC data). In these cases, PPG data do not require any downsampling and the PPG+ACC block is replaced by a PPG-only block (see Fig. 1)⁴.

³PPG data are sampled at a double sampling frequency compared to ACC. Hence, PPG is downsampled before data-level integration with ACC (PPG-only inputs would correspond to 1 channel, 512 samples)

⁴with the 4×256 input for the PPG+ACC block being replaced by a 1×512 input of raw PPG data

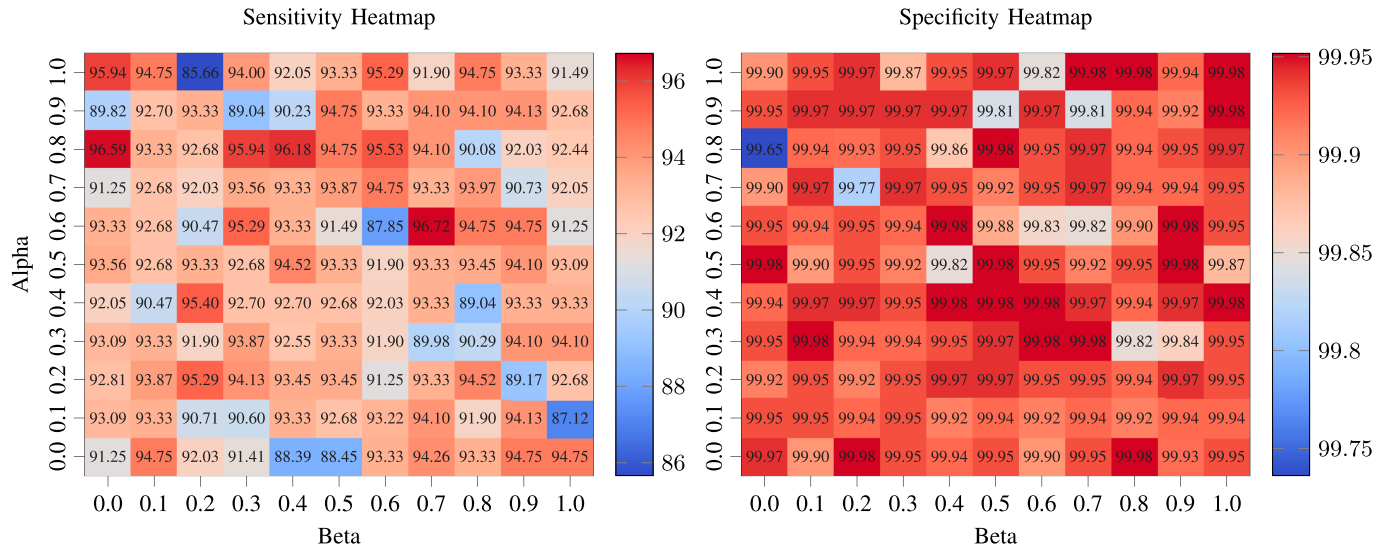


Fig. 2. Heatmaps of sensitivity and specificity for patient 01 of the CHB-MIT dataset, for varying alpha and beta parameters of the SSCWE applied to EPIDENET.

H. Embedded Implementation

We target the GAP9 platform for the model deployment. GAP9 represents the latest commercial evolution in the PULP processor series, distinguished by its enhanced energy efficiency [65]. We select GAP9 in light of its energy efficiency and computational capabilities within the desired power range of milliwatts, which demonstrated state-of-the-art performance for tiny Machine Learning applications [66]. Notably, the GAP9 demonstrates a performance improvement of at least an order of magnitude over traditional single-core low-power processors like the ARM CORTEX M4, all within a comparable power budget [21].

The GAP9 platform offers low-power, parallel computation capabilities with ten cores, based on the RISC-V RV32IMF Instruction Set Architecture, augmented with custom Xpulp extensions for enhanced digital signal processing [65]. The architecture of GAP9 divides these cores into a Fabric Controller (1 core) and Cluster Cores (9 cores). Additionally, the processor is equipped with 128 kB of L1 memory and 1.5 MB of RAM, facilitating the implementation of relatively large models. The cluster cores can operate at speeds up to 370 MHz and collectively utilize 4 Floating-Point Units. These units support a range of numerical formats, including bfloat, FP16, FP32, and selected instructions in FP64, thus offering a versatile environment for computational tasks.

We leverage GAP9 for the deployment of BRAINFUSENET. The BRAINFUSENET computation is divided into distinct sequential phases, focusing on the EEG and PPG/ACC sub-networks, respectively (see Fig. 1). For each phase, we use eight cores for parallel computation and one core for Direct Memory Access. The outcomes from these networks are then summed into a feature vector, which is then forwarded to a fully connected neural layer tasked with generating the final predictive decision. This sequential approach provides flexibility, allowing for adjustments and improvements to individual EPIDENET

modules (the EEG one or the PPG+ACC one) without adversely affecting the performance or computational efficacy of the other component.

To deploy BRAINFUSENET on GAP9, we employ Quantlab [67] for converting to an INT-8 format and use DORY [68] for deployment. DORY is designed to automatically produce C code that handles the two-level memory architecture (L1 and L2 memory) on PULP-based platforms.

I. Energy Measurements

The energy measurements are performed using the GAP9 Evaluation Kit, interfaced with a Power Profiler Kit II (PPK2) that supplies 1.8V, while an on-chip DC-DC converter generates the required 0.65V for the processor. Power consumption is assessed via the PPK2, which provides power to the Evaluation Kit and records current consumption. To ensure consistent measurements across trials, digital pins from the PPK2 are connected to the evaluation board's GPIO pin with a common ground. The reported performance metrics are derived from the mean of ten measurements.

IV. RESULTS

A. EEG-Based Seizure Detection via SSCWE

Our previous publication [60] demonstrated the efficacy of the SSWCE in enhancing result accuracy on the PEDESITE dataset. Here we further expand the analysis, by optimizing the parameters α and β also on the CHB-MIT dataset. We perform a LOOCV subject-specific training, adjusting the α and β parameters within the range of 0 to 1. Fig. 2 shows an example heatmap delineating the variations in sensitivity and specificity for patient 01 of the CHB-MIT dataset. After performing a similar analysis across all patients (see Table II), the optimal combination of α and β parameters was determined on a subject-specific basis. This optimization (compared to using

TABLE II
RESULTS OF EEG-BASED SEIZURE DETECTION ON THE
CHB-MIT AND PEDESITE DATASETS EMPLOYING SSWCE

Patient	α	β	Sens [%]	Spec [%]	FP/h
chb01	0.6	0.9	94.75	99.98	0.14
chb02	0.8	0.8	91.92	100.00	0.00
chb03*	0.0	0.0	86.86	99.89	1.01
chb04	0.3	0.2	68.21	99.78	2.82
chb05	1.0	0.8	95.67	100.00	0.00
chb06	0.6	0.2	30.51	100.00	0.00
chb07	1.0	0.2	79.76	100.00	0.00
chb08	0.1	0.9	89.19	99.50	4.46
chb09	1.0	0.9	92.99	99.74	2.34
chb10*	0.0	0.0	97.95	100.00	0.00
chb11	0.9	1.0	99.11	100.00	0.00
chb12	0.1	0.7	75.28	99.87	1.19
chb13	0.3	0.2	47.43	99.94	0.58
chb14	0.0	1.0	50.24	100.00	0.00
chb15	0.6	0.4	94.15	99.84	1.45
chb16	0.1	0.5	20.00	100.00	0.00
chb17	0.7	1.0	52.22	100.00	0.00
chb18	0.5	0.2	76.20	99.59	3.65
chb19	1.0	0.3	82.72	99.40	5.42
chb20	0.7	1.0	87.33	99.33	6.05
chb21	1.0	0.4	95.00	99.87	1.17
chb22	0.2	0.7	90.74	100.00	0.00
chb23	0.1	0.7	74.25	99.72	2.53
chb24	0.5	0.1	59.72	99.93	0.59
Average	0.50	0.55	76.34	99.85	1.39
P1	0.3	0.7	25.20	99.62	1.71
P2	0.7	0.1	59.44	100.00	0.00
P3	1.0	0.2	65.45	99.67	1.48
P4	0.1	0.5	77.86	99.78	0.99
P5	0.5	0.4	92.50	100.00	0.00
P6	0.3	0.5	43.49	99.36	2.88
Average	0.48	0.4	60.66	99.74	1.18

*when $\alpha = \beta = 0$, the loss function corresponds to the normal CE Loss

the default values of [60]) yields a significant performance enhancement: the average sensitivity increases to 76.34% (corresponding to an increase of 7.61%), the number of detected seizures increases from 169/185 to 173/185, the specificity increases by 0.10%, the false positive per hour (FP/h) rate decreases to 1.39 FP/h (corresponding to a decrease of 62%). The remaining false positives are primarily attributed to artifacts. To further reduce the incidence of false positives, we recommend integrating an artifact detector similar to the one proposed in [36], [69].

B. Wrist-Based Seizure Detection

Table III shows the outcomes of the three distinct approaches for seizure detection utilizing wristband data, namely: PPG, PPG fused with ACC, and reconstructed PPG. Patient 1 does not have ACC data; hence, only results for the PPG case are reported. A relatively low sensitivity can be observed for all methods, with a maximum of approximately 20 – 32% for Patient 3, revealing a potential advantage in integrating ACC data with PPG data at the data level. The average sensitivity values are below 10%, with FP/h reaching a minimum of 5.3 FP/h for the PPG-ACC fused case. These findings suggest that wrist-worn

TABLE III
RESULTS OF WRIST-BASED SEIZURE DETECTION ON THE PEDESITE
DATASET ACROSS DIFFERENT PATIENTS (P1-P6)

		P1*	P2	P3	P4	P5	P6	Avg
PPG	Sens [%]	3.3	0	3.8	23.1	8.1	2.5	6.8
	Spec [%]	98.4	99.4	97.4	99.4	95	98.4	98.0
	FP/h	7.2	2.6	11.7	2.7	22.5	7.1	9.0
Fused PPG	Sens [%]	-	0	4.1	32	2.1	2.6	8.2
	Spec [%]	-	99.4	98.5	99.9	97.9	98.4	98.8
	FP/h	-	2.7	6.8	0.5	9.5	7.2	5.3
PPG Recon	Sens [%]	-	0	6.1	20	2.7	3.6	8.1
	Spec [%]	-	99.5	98.0	99.4	96.6	98.3	98.1
	FP/h	-	2.3	9.0	2.6	15.2	7.7	8.6

(* Patient P1 does not have ACC data)

TABLE IV
SENSOR FUSION OF EEG+WRIST DATA ON THE PEDESITE DATASET

Data	Fusion	Type	Sens [%]	Spec [%]	FP/h
EEG+PPG	Early	Sum	57.05	99.71	1.31
		Concat.	59.22	99.51	2.21
EEG+PPG	Late	Sum	54.42	99.52	2.16
		Rule	49.70	99.70	1.35
EEG+wrist	Early	Sum	61.21	99.82	0.81
		Concat.	61.23	99.63	1.67
EEG+wrist	Late	Sum	55.32	99.61	1.76
		Rule	50.12	99.72	1.26

sensors may be mostly suitable for subjects exhibiting cardiac variations concomitant with seizure episodes, as demonstrated in the case of Patient 3, whose results are consistent with the performance of alternative PPG-based seizure detection results reported in the literature [54] (32% average sensitivity). Despite the poor performance when wrist data are used in isolation (for this specific dataset), the capability of PPG to detect a minimum number of seizure events shows potential to boost the performance of EEG-based classifications (via sensor fusion – next section).

C. Sensor Fusion

Table IV presents the results of the different sensor fusion methodologies when considering EEG and wrist data.

In Early Fusion scenarios, the concatenation fusion type shows enhanced sensitivity, whereas Weighted Summation performs better in specificity (99.51% vs. 99.71%). For Late Fusion techniques, Rule-Based Fusion outperforms Weighted Summation in specificity (99.70% vs. 99.52%), albeit with lower sensitivity (49.70% vs 54.42%). Overall, Early Fusion approaches yield superior results, both for EEG+PPG and for EEG+PPG+ACC, achieving a balance of sensitivity (59.22%) and specificity (99.71%) and a minimum in the false positives per hour (1.31 FP/h for EEG+PPG, 0.81 FP/h for EEG+PPG+ACC).

Starting from these results, Table V shows a performance comparison across different data processing pipelines, all based

TABLE V
SEIZURE DETECTION RESULTS FOR EEG-ONLY AND (EARLY, SUMMATION-BASED) SENSOR FUSION (EEG+PPG AND EEG+PPG+ACC) ON THE PEDESITE DATASET, FOR DIFFERENT LOSS FUNCTIONS (CE OR SSWCE) AND CONSIDERING SMOOTHED CLASSIFICATION OUTPUTS

Patient	EEG CE			EEG (Smooth) SSWCE			EEG+PPG (Smooth) SSWCE			EEG+PPG+ACC (Smooth) SSWCE		
	Sens [%]	Spec [%]	FP/h	Sens [%]	Spec [%]	FP/h	Sens [%]	Spec [%]	FP/h	Sens [%]	Spec [%]	FP/h
P1	9.70	99.52	2.16	25.20	99.62	1.71	22.90	99.76	1.08	-	-	-
P2	57.00	100	0	59.44	100	0	59.10	100	0	46.31	99.98	0.11
P3	68.20	99.48	2.34	65.45	99.67	1.48	69.95	99.56	1.98	60.07	99.95	0.24
P4	73.40	99.72	1.26	77.86	99.78	0.99	82.29	99.82	0.81	77.95	99.85	0.68
P5	91.10	99.82	0.81	92.50	100	0	91.24	100	0	91.06	100	0
P6	48.70	96.90	14.0	43.49	99.36	2.88	41.81	99.50	2.15	46.03	100	0
Average	58.02	99.24	3.43	60.66	99.74	1.18	61.22	99.77	1.00	64.28	99.96	0.21

TABLE VI
SUMMARY OF SCALP EEG-BASED SEIZURE DETECTION PROCESSING STATE-OF-THE-ART FOR LOW (<8) CHANNEL COUNT

Work	Dataset	Length	Window	Subjects	Channels	Algorithm	Sample Metrics			Event Metrics	
							Sens.	Spec.	FP/h	Sens. [†]	FP/day
[8]	CHB-MIT	944h	4s	23	2	RF	96.6%	92.2%	-	-	-
[50]	UZ Leuven	5284h	2s	54	4	SVM	63.4%	-	0.9	-	-
[51]	CHB-MIT	464h	8s	8	4	Transformer	65.5%	99.9%	0.8	73%	-
[52]	PEDESITE	944h	8s	6	4	Transformer	50.2%	99.7%	-	88%	10.8
[71]	EPILEPSIAE	4603h	3s	29	3	CNN	87.0%	95.7%	52.0	-	-
[47]	CHB-MIT	944h	1s	23	5	RF	99.8%	99.8%	4.3	-	-
This Work	CHB-MIT	944h	4s	24	4	EpiDeNET	76.34%	99.85%	1.39	93.5%	5.80*
This Work	PEDESITE	591h	8s	6	4 + 4 (EEG+PPG/ACC)	BRAINFuseNET	64.28%	99.96%	0.21	95%	0.58*

[†]detected seizure events, *event-based FP/day are calculated as in [70].

on the early fusion (summation) approach. Specifically, we evaluate:

- EEG alone (EpiDeNET) with standard cross-entropy (CE) loss;
- EEG alone (EpiDeNET) with the SSWCE and a three-window majority smoothing;
- Sensor fusion (BRAINFuseNET) between EEG and PPG, with SSWCE and a three-window majority smoothing;
- Sensor fusion (BRAINFuseNET) between EEG and PPG+ACC, with SSWCE and a three-window majority smoothing.

According to Table V, the integration of wrist data improves both specificity and sensitivity. Specifically, starting from the EEG-only results of EpiDeNET, integrating PPG data increases the sensitivity from 60.66% to 61.22% and the false positive rate drops from 1.18 FP/h to 1.00 FP/h. The integration of both PPG and ACC data yields further improvements, with the sensitivity reaching 64.28% and the false positive rate being as low as only 0.21 FP/h. These results demonstrate the importance of performing measurements via heterogeneous sensors.

D. Comparison to State-of-the-Art

Table VI compares the performance of EpiDeNET and BRAINFUSENET to state-of-the-art seizure detection based on low (< 8) channel count. Considering the CHB-MIT dataset, EpiDeNET achieves a lower false positive rate, while retaining

an ability to detect a number of seizure events as high as 93.5% (Sensitivity column in the event metrics). While Busia et al. [51] achieves an even lower FP/h rate (0.8 FP/h, compared to 1.39 FP/h for EpiDeNET), this number was obtained only from a subset (8 subjects) of the total number of patients of the dataset.

Considering the PEDESITE dataset, BRAINFUSENET also outperforms state-of-the-art, currently represented by the EEG-former model of Busia et al. [52]. In fact, BRAINFUSENET achieves a lower false positive rate (0.21 FP/h, compared to 1.35 FP/h) and an increased number of detected seizure events (92%, compared to 88%).

Finally, Table VI (last column) also reports event-based calculation of false positives (following the methodology of [70], where adjacent windows flagged as false positive are marked as a single common false alarm event), and showcases that BRAINFUSENET achieves less than one false alarm per day.

E. Embedded Implementation

We deploy BRAINFUSENET on the GAP9 platform utilizing an 8-second input window. The power consumption trace for this duration is illustrated in Fig. 3, and a comparative analysis of the deployed network against existing studies is presented in Table VII. The inference procedure is executed within a timeframe of 5.56 milliseconds for the EEG+PPG+ACC configuration and 6.29 milliseconds for the EEG+PPG configuration.

TABLE VII
IMPLEMENTATION OF BRAINFUSENET ON GAP9 AND COMPARISON TO RELATED WORKS

Network Data	BRAINFUSENET* EEG+PPG	BRAINFUSENET* EEG+PPG+ACC	[52] EEG	[51] EEG	[41] EEG
Platform	GAP9	GAP9	GAP9	Apollo 4	nRF52840
MCU	1+9×RISCY @240 MHz	1+9×RISCY @240 MHz	1+9×RISCY @240 MHz	1×Cortex M4F @96 MHz	1×Cortex M4F @64 MHz
Deployment framework	Quantlab/DORY	Quantlab/DORY	Quantlab/DORY	Quantlab/CMSIS-NN	TFLite
Dataset	PEDESITE	PEDESITE	PEDESITE	CHB-MIT	CHB-MIT
Input size	4 × 2048 1 × 512	4 × 2048 4 × 256	4 × 2048	4 × 2048	9 × 256
MACs	2 265 616	2 293 696	7 350 000	6 250 000	2 400 000
Time/inference [ms]	6.29	5.56	13.7	405.00	100
Throughput [MMAC/s]	360.19	412.54	536.49	15.43	24
MACs/cycle	1.50	1.72	2.24	0.16	0.38
Power [mW]	18.69	19.25	22.9	4.40	1.5
Energy/inference [mJ]	0.12	0.11	0.31	1.79	0.15
En. eff. [GMAC/s/W]	19.27	21.43	23.42	3.51	16.00

*See Fig. 1 for the architectural differences when using only PPG or both PPG and ACC for wrist data

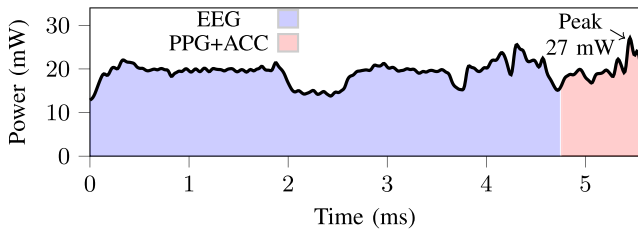


Fig. 3. Power trace of BRAINFUSENET implemented on GAP9.

The EEG component of BRAINFUSENET requires a longer execution time, and we attribute this to the increased data volume processed within this network segment (2048 samples per EEG channel vs. 256 samples per wrist channel). Specifically, within the EEG+PPG+ACC configuration of BRAINFUSENET, the EEG portion requires approximately 4.69 milliseconds, whereas the PPG+ACC components are executed in less than 0.85 milliseconds (the remaining time corresponds to the FCN layer at the end of the network). The peak power consumption is 27 mW: it is observed when processing the final convolutional layer in the PPG+ACC network. The mean power consumption is 19.25 mW, and it corresponds to a total energy consumption of only 0.11 mJ per inference.

Integrating the GAP9 implementation with a state-of-the-art commercial analog front end for biosignal acquisition, such as the widely used Texas Instruments ADS1298 (as used in [72]), which requires 0.75 milliwatts per channel, and considering a battery capacity of 300 mAh, our approach is projected to enable approximately 300 hours of continuous online data acquisition and classification at 8-second intervals. This configuration offers the potential for multi-day continuous monitoring without recharging or battery replacement.

V. CONCLUSION

We presented BRAINFUSENET, a lightweight seizure detection network tailored for wearable devices with a limited

number of sensor channels and exploiting heterogeneous signal sources. BRAINFUSENET is based on the sensor fusion of EEG and wrist-based signals (PPG and accelerometers) and achieves high sensitivity and specificity rates, with 93.5% and 95% event-based seizures correctly detected on the CHB-MIT and PEDESITE datasets, respectively. At the same time, BRAINFUSENET offers state-of-the-art performance in terms of false positive rate, which is as low as 0.21 FP/h. When subsequent sample windows classified as false positives detection are considered as a single event (as in [70]), BRAINFUSENET results in less than one false alarm per day, thereby making it well suited for user's acceptance [35].

These results have been achieved starting from the EPIDENET network, as originally conceived for EEG signals, thanks to a novel Sensitivity-Specificity Weighted Cross Entropy (SS-WCE) loss, which demonstrated its effectiveness in tackling the prevalent issue of class imbalance within seizure datasets, and thanks to sensor fusion across heterogeneous signal sources.

The deployment of BRAINFUSENET on the GAP9 platform demonstrated its suitability for real-world applications, thanks to an energy efficiency of 21.43 GMAC/s/W, a per-inference energy consumption of just 0.11 mJ, and a total average power consumption as low as 19.25 mW.

In summary, this paper highlights the crucial role of sensor fusion in enhancing the robustness and reliability of seizure detection systems. By effectively combining EEG and wrist data, BRAINFUSENET not only improves seizure detection rates and reduces false positives, but also paves the way for more personalized, robust, and adaptable monitoring solutions.

REFERENCES

- [1] World Health Organization, "Epilepsy: A public health imperative," 2019 [Online]. Available: <https://www.who.int/publications/i/item/epilepsy-a-public-health-imperative>
- [2] A. T. Berg, "Identification of pharmacoresistant epilepsy," *Neurologic Clinics*, vol. 27, no. 4, pp. 1003–1013, 2009.
- [3] L. Walker, N. Mirza, V. Yip, A. Marson, and M. Pirmohamed, "Personalized medicine approaches in epilepsy," *J. Internal Med.*, vol. 277, no. 2, pp. 218–234, 2015.

- [4] S. Beniczky et al., "Standardized computer-based organized reporting of EEG: SCORE—Second version," *Clin. Neurophysiol.*, vol. 128, no. 11, pp. 2334–2346, 2017.
- [5] C. E. Elger and C. Hoppe, "Diagnostic challenges in epilepsy: Seizure under-reporting and seizure detection," *Lancet Neurol.*, vol. 17, no. 3, pp. 279–288, 2018.
- [6] P. Ryvlin et al., "Incidence and mechanisms of cardiorespiratory arrests in epilepsy monitoring units (MORTEMUS): A retrospective study," *Lancet Neurol.*, vol. 12, no. 10, pp. 966–977, 2013.
- [7] I. Hubbard, S. Beniczky, and P. Ryvlin, "The challenging path to developing a mobile health device for epilepsy: The current landscape and where we go from here," *Frontiers Neurol.*, vol. 12, 2021, Art. no. 740743.
- [8] R. Zanetti, A. Aminifar, and D. Atienza, "Robust epileptic seizure detection on wearable systems with reduced false-alarm rate," in *Proc. 42nd Annu. Int. Conf. IEEE Eng. Med. Biol. Soc. (EMBC)*, Piscataway, NJ, USA: IEEE Press, 2020, pp. 4248–4251.
- [9] B. Abbasi and D. M. Goldenholz, "Machine learning applications in epilepsy," *Epilepsia*, vol. 60, no. 10, pp. 2037–2047, 2019.
- [10] E. Bruno et al., "Wearable technology in epilepsy: The views of patients, caregivers, and healthcare professionals," *Epilepsy Behav.*, vol. 85, pp. 141–149, Aug. 2018.
- [11] A. Abdelhameed and M. Bayoumi, "A deep learning approach for automatic seizure detection in children with epilepsy," *Frontiers Comput. Neurosci.*, vol. 15, Apr. 2021. Accessed: Feb. 15, 2024. [Online]. Available: <https://www.frontiersin.org/articles/10.3389/fncom.2021.650050>
- [12] R. S. Fisher et al., "Epileptic seizures and epilepsy: definitions proposed by the International League Against Epilepsy (ILAE) and the International Bureau for Epilepsy (IBE)," *Epilepsia*, vol. 46, no. 4, pp. 470–472, 2005.
- [13] L. Kuhlmann, K. Lehnertz, M. P. Richardson, B. Schelter, and H. P. Zaveri, "Seizure prediction—Ready for a new era," *Nature Rev. Neurol.*, vol. 14, no. 10, pp. 618–630, 2018.
- [14] B. R. Greene, G. B. Boylan, R. B. Reilly, P. de Chazal, and S. Connolly, "Combination of EEG and ECG for improved automatic neonatal seizure detection," *Clin. Neurophysiol.*, vol. 118, no. 6, pp. 1348–1359, 2007.
- [15] N. D. Truong et al., "Convolutional neural networks for seizure prediction using intracranial and scalp electroencephalogram," *Neural Netw.*, vol. 105, pp. 104–111, Sep. 2018.
- [16] J. A. Urigüen and B. Garcia-Zapirain, "Eeg artifact removal—State-of-the-art and guidelines," *J. Neural Eng.*, vol. 12, no. 3, 2015, Art. no. 031001.
- [17] J. W. Britton et al., "Electroencephalography (EEG): An introductory text and atlas of normal and abnormal findings in adults, children, and infants," Chicago, IL, USA: American Epilepsy Society, 2016.
- [18] M. Daneshi Kohan, A. Motie Nasrabadi, M. B. Shamsollahi, and A. Sharifi, "Eeg/ppg effective connectivity fusion for analyzing deception in interview," *Signal, Image Video Process.*, vol. 14, pp. 907–914, Jul. 2020.
- [19] C. Cannard, H. Wahbeh, and A. Delorme, "BrainBeats: An open-source EEG/PPG plugin to jointly analyze EEG and cardiovascular (ECG/PPG) signals," *bioRxiv*, 2023.
- [20] D. Zambrana-Vinaroz, J. M. Vicente-Samper, J. Manrique-Cordoba, and J. M. Sabater-Navarro, "Wearable epileptic seizure prediction system based on machine learning techniques using ECG, PPG and EEG signals," *Sensors*, vol. 22, no. 23, 2022, Art. no. 9372.
- [21] T. M. Ingolfsson et al., "EpiDeNet: An energy-efficient approach to seizure detection for embedded systems," in *Proc. IEEE Biomed. Circuits Syst. Conf.*, 2023, pp. 1–5.
- [22] A. Van de Vel et al., "Long-term home monitoring of hypermotor seizures by patient-worn accelerometers," *Epilepsy Behav.*, vol. 26, no. 1, pp. 118–125, 2013.
- [23] S. Beniczky, I. Conradsen, O. Henning, M. Fabricius, and P. Wolf, "Automated real-time detection of tonic-clonic seizures using a wearable EMG device," *Neurology*, vol. 90, no. 5, pp. e428–e434, 2018.
- [24] D. Cogan, J. Birjandtalab, M. Nourani, J. Harvey, and V. Nagaraddi, "Multi-biosignal analysis for epileptic seizure monitoring," *Int. J. Neural Syst.*, vol. 27, no. 1, 2017, Art. no. 1650031.
- [25] "Empatica health monitor." Empatica. Accessed: Nov. 15, 2023. [Online]. Available: <https://www.empatica.com/research/e4/>
- [26] T. Rukasha, S. I. Woolley, and T. Collins, "Wearable epilepsy seizure monitor user interface evaluation: an evaluation of the empatica 'embrace' interface," in *Adjunct Proc. ACM Int. Joint Conf. Pervasive Ubiquitous Comput./Proc. ACM Int. Symp. Wearable Comput. (UbiComp/ISWC '20 Adjunct)*, New York, NY, USA: ACM, 2020, pp. 110–114, doi: 10.1145/3410530.3414382.
- [27] "I-Brain." Neurovigil. Accessed: Nov. 15, 2023. [Online]. Available: <https://www.neurovigil.com/index.php/technology/ibrain-device>
- [28] SEER MEDICAL. Accessed: Nov. 15, 2023. [Online]. Available: <https://seermedical.com/>
- [29] D. Sopic, A. Aminifar, and D. Atienza, "e-Glass: A wearable system for real-time detection of epileptic seizures," in *Proc. IEEE Int. Symp. Circuits Syst. (ISCAS)*, 2018, pp. 1–5.
- [30] C. Maher, Y. Yang, N. D. Truong, C. Wang, A. Nikpour, and O. Kavehei, "Seizure detection with reduced electroencephalogram channels: Research trends and outlook," *Roy. Soc. Open Sci.*, vol. 10, no. 5, 2023, Art. no. 230022.
- [31] I. Zibrandtsen, P. Kidmose, C. Christensen, and T. Kjaer, "Ear-EEG detects ictal and interictal abnormalities in focal and generalized epilepsy—A comparison with scalp EEG monitoring," *Clin. Neurophysiol.*, vol. 128, no. 12, pp. 2454–2461, 2017. Accessed: Feb. 15, 2024. [Online]. Available: <https://www.sciencedirect.com/science/article/pii/S1388245717310763>
- [32] MJN, "EEG EARBUD." Epilepsy Alarms UK. Accessed: Nov. 15, 2023. [Online]. Available: <https://www.epilepsyalarms.co.uk/product/mjn-seras>
- [33] M. Altini, S. Del Din, S. Patel, S. Schachter, J. Penders, and P. Bonato, "A low-power multi-modal body sensor network with application to epileptic seizure monitoring," in *Proc. Annu. Int. Conf. IEEE Eng. Med. Biol. Soc.*, pp. 1806–1809.
- [34] R. Gravina, P. Alinia, H. Ghasemzadeh, and G. Fortino, "Multi-sensor fusion in body sensor networks: State-of-the-art and research challenges," *Inf. Fusion*, vol. 35, pp. 68–80, 2017.
- [35] J. J. Halford et al., "Detection of generalized tonic-clonic seizures using surface electromyographic monitoring," *Epilepsia*, vol. 58, no. 11, pp. 1861–1869, Nov. 2017.
- [36] T. M. Ingolfsson et al., "Minimizing artifact-induced false-alarms for seizure detection in wearable eeg devices with gradient-boosted tree classifiers," *Sci. Rep.*, vol. 14, no. 1, 2024, Art. no. 2980.
- [37] L. Frølich and I. Dowding, "Removal of muscular artifacts in EEG signals: A comparison of linear decomposition methods," *Brain Inform.*, vol. 5, no. 1, pp. 13–22, 2018.
- [38] B. Al-Sheikh, "Adaptive algorithm for motion artifacts removal in wearable biomedical sensors during physical exercise," *IEEE Sensors J.*, vol. 23, no. 9, pp. 9491–9499, May 2023.
- [39] T. Bermudez, D. Lowe, and A.-M. Arlaud-Lamborelle, "EEG/ECG information fusion for epileptic event detection," in *Proc. 16th Int. Conf. Digit. Signal Process.*, Piscataway, NJ, USA: IEEE Press, 2009, pp. 1–8.
- [40] M.-Z. Poh et al., "Convulsive seizure detection using a wrist-worn electrodermal activity and accelerometry biosensor," *Epilepsia*, vol. 53, no. 5, pp. e93–e97, 2012.
- [41] X. Liu and A. G. Richardson, "Edge deep learning for neural implants: A case study of seizure detection and prediction," *J. Neural Eng.*, vol. 18, no. 4, 2021, Art. no. 046034.
- [42] Y. Liu et al., "Epilepsy detection with artificial neural network based on as-fabricated neuromorphic chip platform," *AIP Adv.*, vol. 12, no. 3, 2022.
- [43] M. Tohidi, J. K. Madsen, and F. Moradi, "A low-power, low-noise, high-accurate epileptic-seizure detection system for wearable applications," *Microelectron. J.*, vol. 92, 2019, Art. no. 104600.
- [44] K. Patel, C.-P. Chua, S. Fau, and C. J. Bleakley, "Low power real-time seizure detection for ambulatory EEG," in *Proc. 3rd Int. Conf. Pervasive Comput. Technol. Healthcare*, Piscataway, NJ, USA: IEEE Press, 2009, pp. 1–7.
- [45] A. Page, C. Sagedy, E. Smith, N. Attaran, T. Oates, and T. Mohsenin, "A flexible multichannel EEG feature extractor and classifier for seizure detection," *IEEE Trans. Circuits Syst. II, Exp. Briefs*, vol. 62, no. 2, pp. 109–113, Feb. 2015.
- [46] T. Zhan, S. Z. Fatmi, S. Guraya, and H. Kassiri, "A resource-optimized VLSI implementation of a patient-specific seizure detection algorithm on a custom-made 2.2 cm² wireless device for ambulatory epilepsy diagnostics," *IEEE Trans. Biomed. Circuits Syst.*, vol. 13, no. 6, pp. 1175–1185, Dec. 2019.
- [47] J. Zeng, X.-d. Tan, and A. Z. Chang'an, "Automatic detection of epileptic seizure events using the time-frequency features and machine learning," *Biomed. Signal Process. Control*, vol. 69, 2021, Art. no. 102916.
- [48] E. I. Shih, A. H. Shoeb, and J. V. Gutttag, "Sensor selection for energy-efficient ambulatory medical monitoring," in *Proc. 7th Int. Conf. Mobile Syst., Appl., Services*, 2009, pp. 347–358.
- [49] L. A. Moctezuma and M. Molinas, "Classification of low-density EEG for epileptic seizures by energy and fractal features based on EMD," *J. Biomed. Res.*, vol. 34, no. 3, 2020, Art. no. 180.

- [50] K. Vandecasteele et al., "Visual seizure annotation and automated seizure detection using behind-the-ear electroencephalographic channels," *Epilepsia*, vol. 61, no. 4, pp. 766–775, 2020.
- [51] P. Busia et al., "EEGformer: Transformer-based epilepsy detection on raw EEG traces for low-channel-count wearable continuous monitoring devices," in *Proc. IEEE Biomed. Circuits Syst. Conf.*, 2022, pp. 640–644.
- [52] P. Busia et al., "Reducing false alarms in wearable seizure detection with EEGformer: A compact transformer model for MCUs," *IEEE Trans. Biomed. Circuits Syst.*, early access, Jan. 23, 2024.
- [53] F. Mohammadpour Touserani et al., "Photoplethysmographic evaluation of generalized tonic-clonic seizures," *Epilepsia*, vol. 61, no. 8, pp. 1606–1616, 2020.
- [54] K. Vandecasteele et al., "Automated epileptic seizure detection based on wearable ECG and PPG in a hospital environment," *Sensors*, vol. 17, no. 10, 2017, Art. no. 2338.
- [55] T.-Y. Lin, P. Goyal, R. Girshick, K. He, and P. Dollár, "Focal loss for dense object detection," in *Proc. IEEE Int. Conf. Comput. Vis.*, 2017, pp. 2980–2988.
- [56] S. Wang, W. Liu, J. Wu, L. Cao, Q. Meng, and P. J. Kennedy, "Training deep neural networks on imbalanced data sets," in *Proc. Int. Joint Conf. Neural Netw.*, Piscataway, NJ, USA: IEEE Press, 2016, pp. 4368–4374.
- [57] N. V. Chawla, K. W. Bowyer, L. O. Hall, and W. P. Kegelmeyer, "SMOTE: Synthetic minority over-sampling technique," *J. Artif. Intell. Res.*, vol. 16, pp. 321–357, Jun. 2002.
- [58] C. Drummond et al., "C4. 5, class imbalance, and cost sensitivity: Why under-sampling beats over-sampling," in *Proc. Workshop Learn. Imbalanced Datasets II*, vol. 11, 2003, pp. 1–8.
- [59] A. L. Goldberger et al., "PhysioBank, PhysioToolkit, and PhysioNet," *Circulation*, vol. 101, no. 23, pp. e215–e220, Jun. 2000, doi: 10.1161/01.CIR.101.23.e215.
- [60] T. M. Ingolfsson et al., "Towards long-term non-invasive monitoring for epilepsy via wearable EEG devices," in *Proc. IEEE Biomed. Circuits Syst. Conf. (BioCAS)*, 2021, pp. 01–04.
- [61] G. P. Nason and B. W. Silverman, "The stationary wavelet transform and some statistical applications," in *Wavelets and Statistics*. New York, NY, USA: Springer-Verlag, 1995, pp. 281–299.
- [62] W. Chen, N. Jaques, S. Taylor, A. Sano, S. Fedor, and R. W. Picard, "Wavelet-based motion artifact removal for electrodermal activity," in *Proc. 37th Annu. Int. Conf. IEEE Eng. Med. Biol. Soc. (EMBC)*, 2015, pp. 6223–6226.
- [63] S. Nasehi and H. Pourghassem, "Real-time seizure detection based on EEG and ECG fused features using Gabor functions," in *Proc. Int. Conf. Intell. Comput. Bio-Med. Instrum.*, Piscataway, NJ, USA: IEEE Press, 2011, pp. 204–207.
- [64] L.-M. Vortmann, S. Ceh, and F. Putze, "Multimodal EEG and eye tracking feature fusion approaches for attention classification in hybrid BCIs," *Frontiers Comput. Sci.*, vol. 4, 2022, Art. no. 780580.
- [65] D. Rossi et al., "Vega: A ten-core SoC for IoT endnodes with DNN acceleration and cognitive wake-up from MRAM-based state-retentive sleep mode," *IEEE J. Solid-State Circuits*, vol. 57, no. 1, pp. 127–139, Jan. 2022.
- [66] "Inference: tiny. v1.0 results." ML Commons. Accessed: Nov. 15, 2023. [Online]. Available: <https://mlcommons.org/en/inference-tiny-10/>
- [67] M. Spallanzani, G. Rutishauser, M. Scherer, A. Burrello, F. Conti, and L. Benini, "QuantLab: A modular framework for training and deploying mixed-precision NNs," tinyML Foundation. Accessed: Feb. 15, 2024. [Online]. Available: <https://cms.tinyml.org/wp-content/uploads/talks2022/Spallanzani-Matteo-Hardware.pdf>
- [68] A. Burrello, A. Garofalo, N. Bruschi, G. Tagliavini, D. Rossi, and F. Conti, "DORY: Automatic end-to-end deployment of real-world DNNs on low-cost IoT MCUs," *IEEE Trans. Comput.*, vol. 70, no. 8, pp. 1253–1268, Aug. 2021.
- [69] T. M. Ingolfsson, A. Cossetini, S. Benatti, and L. Benini, "Energy-efficient tree-based EEG artifact detection," in *Proc. 44th Annu. Int. Conf. IEEE Eng. Med. Biol. Soc. (EMBC)*, 2022, pp. 3723–3728.
- [70] J. Dan et al., "SzCORE: A seizure community open-source research evaluation framework for the validation of EEG-based automated seizure detection algorithms," 2024, *arXiv:2402.13005v3*.
- [71] S. Baghersalimi, A. Amirshahi, F. Forooghifar, T. Teijeiro, A. Aminifar, and D. Atienza, "Many-to-one knowledge distillation of real-time epileptic seizure detection for low-power wearable Internet of Things systems," 2022, *arXiv:2208.00885*.
- [72] S. Frey, M. Guermendi, S. Benatti, V. Kartsch, A. Cossetini, and L. Benini, "BioGAP: A 10-core FP-capable ultra-low power IoT processor, with medical-grade AFE and BLE connectivity for wearable biosignal processing," in *Proc. IEEE Int. Conf. Omni-Layer Intell. Syst. (COINS)*, Piscataway, NJ, USA: IEEE Press, 2023, pp. 1–7.



Thorir Mar Ingolfsson (Graduate Student Member, IEEE) received the bachelor's degree in electrical and computer engineering from the University of Iceland, in 2018, and the master's degree in electrical engineering and information technology from the ETH Zürich, Switzerland, in 2020. Currently, he is working toward the Ph.D. degree with the ETH Zürich, working under the supervision of Prof. Dr. Luca Benini with the Integrated Systems Laboratory. His research interests include biosignal processing and machine learning, emphasizing low-power embedded systems, and energy-efficient implementation of machine learning models on microcontrollers.



Xiaying Wang (Member, IEEE) received the B.Sc. and M.Sc. degrees in biomedical engineering from the Politecnico di Milano, Italy, and the ETH Zurich, Switzerland, in 2016 and 2018, respectively, and the Ph.D. degree in electrical engineering from the ETH Zurich, Switzerland, in 2023 (Doctor of Science ETH). She won the Ph.D. Fellowship funded by the Swiss Data Science Center, in 2019. She is currently a Postdoctoral Researcher with the Integrated Systems Laboratory, ETH Zurich and with Swiss University of Traditional Chinese Medicine in Switzerland. Her research interests include biosignal processing, brain-machine interface, smart wearable devices, edge computing, and applied machine learning.



Upasana Chakraborty received the bachelor's degree in electronics and communication from the Birla Institute of Technology, Pilani, in 2018, and the master's degree in electrical engineering and information technology from the ETH Zürich, Switzerland, in 2023. She pursued her master's thesis under the supervision of Prof. Dr. Luca Benini with the Integrated Systems Laboratory.



Simone Benatti (Member, IEEE) received the Ph.D. degree in electronics, telecommunications and information technologies from the University of Bologna, under the supervision of Prof. Luca Benini. During the Ph.D., he was a Visiting Fellow with BWRC – University of California, Berkeley (Supervisor Prof. Jan Rabaey). Currently, he serves as an Assistant Professor with the University of Modena e Reggio Emilia, while pursuing his collaboration with EEES Lab, Bologna. In 2023, he has been appointed as a Visiting Professor with EFCL-ETHZ. His research interests include energy-efficient embedded systems for IoT and biomedical applications. This includes hardware/software codesign to efficiently address performance, as well as advanced algorithms. He works on designing and optimizing energy-efficient embedded systems for biopotential (EMG and EEG) acquisition and processing, and on brain-machine interface for HMI. In this field, he has published more than 90 papers in international peer-reviewed conferences and journals. He has ongoing collaborations with several international research institutes, such as ETHZ-EFCL, EPFL, TU Graz, FBK and Politecnico di Torino. He is a recipient of the GHAIIA Grant (H2020-MSCA-RISE-2017, G.A. 777822).



Adriano Bernini received the Ph.D. degree in neurosciences with the Lemanic Neuroscience Doctoral School from the University of Lausanne, Lausanne, Switzerland, in 2022, focusing on clinical neuroscience and brain metabolism at the acute phase following brain injury in human. In 2022, he joined with the NeuroTech Group, Department of Clinical Neuroscience, Lausanne University Hospital (CHUV) as a Post-Doc and Clinical Study Manager. His research interests include epilepsy disease together with the use of connected wearable devices

to develop seizures detection algorithms.



Pauline Ducouret received the Ph.D. degree in life sciences from the Université of Lausanne, Lausanne, Switzerland, in 2019. She joined with Department of Clinical Neuroscience, Lausanne University Hospital (CHUV) as a Post-Doc, Clinical Study Manager, and Data Manager, in 2021. Her research interests include migraine and epilepsy diseases and the use of connected wearable devices to develop detection algorithms.



Philippe Ryvlin is a Full Professor with UNIL and Head of the Department of Clinical Neurosciences, CHUV, since 2015, and an Affiliated Professor with the University of Copenhagen. His research using connected objects in the field of epilepsy aims to better understand and prevent sudden unexpected death in epilepsy, one of the most frequent causes of sudden death in young adults. His research using mobile health technologies, extends to other neurological diseases.



Sándor Beniczky received the M.D. and Ph.D. degrees. He is a Board-Certified Neurologist, Clinical Neurophysiologist, and Epileptologist. He is a Professor with Aarhus University Hospital, and the Head of the Clinical Neurophysiology Department, Danish Epilepsy Centre. His research interests include EEG and epilepsy, focusing on electromagnetic source imaging, seizure detection, automated and semi-automated analysis, artificial intelligence, standardisation and quality-assurance in clinical neurophysiology. He is an Editor-in-

Chief of *Epileptic Disorders*. He was the Founding Co-Chair of the ILAE Neurotechnology Section.



Luca Benini (Fellow, IEEE) received the Ph.D. degree from the Stanford University, Stanford, CA, USA, in 1997. He holds the Chair of digital circuits and systems with the ETHZ, Zürich, Zürich, Switzerland, and a Full Professor with the Università di Bologna, Bologna, Italy. His research interests are in energy-efficient parallel computing systems, smart sensing micro-systems and machine learning hardware. He is a Fellow of the ACM and a member of the Academia Europaea. He is the recipient of the 2016 IEEE CAS Mac Van

Valkenburg award, the 2020 EDAA achievement Award, the 2020 ACM/IEEE A. Richard Newton Award and the 2023 IEEE CS E.J. McCluskey Award.



Andrea Cossetti (Member, IEEE) received the Ph.D. degree in electronic engineering from the University of Udine, Udine, Italy, in 2019, working on nanoelectrode array biosensors. Previously, he was with Acreo Swedish ICT AB (Kista, Sweden), designing waveguide-to-chip transitions at sub-mm waves, and with Infineon Technologies (Villach, Austria), working on signal integrity for high-speed serial interfaces. He joined with the ETH Zurich, in 2019. His research interests include biomedical circuits and systems, with a special focus on

wearable/high-speed ultrasound and wearable EEG. He currently serves as a Research Cooperation Manager with the ETH Future Computing Laboratory (EFCL), a Project Leader with the Integrated Systems Laboratory, and a Lecturer.